Title

O Antigen Modulates Insect Vector Acquisition of the Bacterial Plant Pathogen Xylella fastidiosa

Journal

Applied and Environmental Microbiology, 81(23)

ISSN

0099-2240

Authors

Rapicavoli, Jeannette N
Kinsinger, Nichola
Perring, Thomas M
et al.

Publication Date

2015-12-01

DOI

10.1128/aem.02383-15

Peer reviewed

AEM
Journals.ASM.org

O Antigen Modulates Insect Vector Acquisition of the Bacterial Plant Pathogen *Xylella fastidiosa*

Jeannette N. Rapicavoli,[a] Nichola Kinsinger,[b] Thomas M. Perring,[c] Elaine A. Backus,[d] Holly J. Shugart,[e] Sharon Walker,[b] M. Caroline Roper[a]

Department of Plant Pathology and Microbiology, University of California, Riverside, California, USA[a]; Department of Chemical and Environmental Engineering, University of California, Riverside, California, USA[b]; Department of Entomology, University of California, Riverside, California, USA[c]; USDA, Agricultural Research Service, USDA-ARS San Joaquin Valley Agricultural Sciences Center, Parlier, California, USA[d]; Department of Entomology, Citrus Research and Education Center, University of Florida, Lake Alfred, Florida, USA[e]

Hemipteran insect vectors transmit the majority of plant pathogens. Acquisition of pathogenic bacteria by these piercing/sucking insects requires intimate associations between the bacterial cells and insect surfaces. Lipopolysaccharide (LPS) is the predominant macromolecule displayed on the cell surface of Gram-negative bacteria and thus mediates bacterial interactions with the environment and potential hosts. We hypothesized that bacterial cell surface properties mediated by LPS would be important in modulating vector-pathogen interactions required for acquisition of the bacterial plant pathogen *Xylella fastidiosa*, the causative agent of Pierce's disease of grapevines. Utilizing a mutant that produces truncated O antigen (the terminal portion of the LPS molecule), we present results that link this LPS structural alteration to a significant decrease in the attachment of *X. fastidiosa* to blue-green sharpshooter foreguts. Scanning electron microscopy confirmed that this defect in initial attachment compromised subsequent biofilm formation within vector foreguts, thus impairing pathogen acquisition. We also establish a relationship between O antigen truncation and significant changes in the physiochemical properties of the cell, which in turn affect the dynamics of *X. fastidiosa* adhesion to the vector foregut. Lastly, we couple measurements of the physiochemical properties of the cell with hydrodynamic fluid shear rates to produce a Comsol model that predicts primary areas of bacterial colonization within blue-green sharpshooter foreguts, and we present experimental data that support the model. These results demonstrate that, in addition to reported protein adhesin-ligand interactions, O antigen is crucial for vector-pathogen interactions, specifically in the acquisition of this destructive agricultural pathogen.

Insect vectors transmit numerous pathogens to a wide range of animal and plant hosts. Hemipteran vectors, such as aphids, leafhoppers, and whiteflies, are an economically important group of insects because they are the dominant vectors of plant pathogens (1). The molecular determinants of transmission have been explored for only a few phytopathosystems (compared to mammalian systems), with virus-vector interactions being the most extensively studied. Surface entities, such as virion capsid components, have been shown to be important for the retention and transmission of plant viruses (2), indicating the importance of pathogen surface properties in mediating these interactions. However, we have much less information regarding the molecular mechanisms of insect transmission of bacterial pathogens, specifically those infecting plants.

Xylella fastidiosa is a Gram-negative bacterium that causes diseases in several economically important crops, including Pierce's disease (PD) of grapevines, citrus variegated chlorosis, and almond leaf scorch. *X. fastidiosa* forms biofilms within the xylem vessels of plant hosts, which occludes vessels and impedes water flow within the vine (3). Symptoms of PD include marginal leaf necrosis, premature leaf abscission, fruit desiccation, and ultimately plant death (3). *X. fastidiosa* is obligately transmitted by xylem-feeding insects primarily belonging to the hemipteran family Cicadellidae, subfamily Cicadellinae, termed sharpshooters (3). The association of *X. fastidiosa* with its insect vectors is unique, in that it is the only known insect-transmitted plant pathogen that is persistent but noncirculative (4). *X. fastidiosa* is semipersistent in nymphs (i.e., the bacterium is lost after each vector molt) but is persistent in adult vectors (which do not molt) (3, 4). Because *X. fastidiosa* is also propagative within vectors, the insects are able to inoculate the pathogen for months after acquisition from an infected plant (3). Transmission of *X. fastidiosa* consists of three main steps, namely, pathogen acquisition from an infected host plant, multiplication and retention of the pathogen within the vector, and inoculation of the pathogen into a susceptible plant host (5). Upon acquisition, *X. fastidiosa* colonizes the vector foregut by attaching to and forming robust biofilms within the cibarial and precibarial regions of the foregut (5, 6). Cells initially attach laterally and begin to colonize the foregut cuticle by seemingly following the developmental steps of canonical biofilm formation, although the kinetics of biofilm development within vector foreguts are not well understood (6). Interestingly, in the later stages of biofilm formation, the cells become polarly attached to the foregut cuticle, presumably to allow for

Received 24 July 2015 **Accepted** 14 September 2015

Accepted manuscript posted online 18 September 2015

Citation Rapicavoli JN, Kinsinger N, Perring TM, Backus EA, Shugart HJ, Walker S, Roper MC. 2015. O antigen modulates insect vector acquisition of the bacterial plant pathogen *Xylella fastidiosa*. Appl Environ Microbiol 81:8145–8154. doi:10.1128/AEM.02383-15.

Editor: H. Goodrich-Blair

Address correspondence to M. Caroline Roper, mcroper@ucr.edu.

Supplemental material for this article may be found at http://dx.doi.org/10.1128/AEM.02383-15.

maximal surface area exposure to the nutrient-dilute xylem sap that is ingested by the insect (3). Several bacterial components, such as type I pili, hemagglutinin adhesins, and fimbriae, contribute (in various capacities) to different stages of *X. fastidiosa* colonization in sharpshooter vectors (3, 6). Killiny and Almeida examined the contributions of the hemagglutinin adhesins HxfA and HxfB to the transmission process and found that the adhesins were impaired in attachment to nitrocellulose coated with blue-green sharpshooter (BGSS) foregut extracts and transmission rates were low. Interestingly, *hxfA* and *hxfB* mutants multiplied to similar levels, compared with the wild type, in vector foreguts (6). In addition, overall transmission rates for a *fimA* knockout mutant (lacking the type I pilus) were lower than wild-type rates (5). Exopolysaccharide (EPS) has also been implicated in the insect transmission of *X. fastidiosa* by the BGSS *Graphocephala atropunctata* (Signoret) (7). EPS^- mutants were transmitted at significantly lower rates than wild-type *X. fastidiosa* but were not impaired in attachment to nitrocellulose coated with BGSS foregut extracts. This suggests that a lack of EPS does not impair the initial attachment to the insect foregut cuticle but may impair subsequent steps in the insect colonization process (6, 7). Interestingly, mutations in any of these fimbrial/afimbrial adhesins or changes in EPS production never fully compromised the transmissibility of the pathogen, indicating that vector transmission is a complex process that relies on many factors involved in the acquisition, retention, or inoculation of the pathogen. To date, little attention has been given to the predominant bacterial cell surface polysaccharide, i.e., lipopolysaccharide (LPS), and its role in this complex biological process, for any bacterial pathogen-vector relationship.

LPS is a tripartite macromolecule located in the outer membranes of all Gram-negative bacteria (8, 9). There are approximately 3.5 million LPS molecules on the bacterial outer membrane (10), occupying more than 75% of the bacterial cell surface (9, 11). LPS is composed of three parts, i.e., lipid A, which anchors the molecule to the outer membrane, core oligosaccharide, and a terminal O antigen consisting of polysaccharide chains (9, 12). While the lipid A and core portions of the molecule are highly conserved, the O antigen can vary greatly in composition and structure, even within strains of the same bacterial species (11, 13, 14). The O antigen is assembled in the cytoplasm and delivered independently to the periplasm, where it is ligated onto the lipid A-core complex and then translocated to the outer membrane (13). This process is mediated in part by the Wzy polymerase, which catalyzes polymerization of the individual O units that make up the O antigen chain (13). Our research group demonstrated previously that the O antigen of wild-type *X. fastidiosa* is a high-molecular-weight polymer consisting of rhamnose-rich O units. In addition, targeted mutation of the Wzy polymerase resulted in a truncated O antigen that was primarily depleted of rhamnose. The *wzy* mutant strain was significantly impaired in production of the O antigen component of LPS, compared with the wild type, which was clearly visible when purified LPS was analyzed on a discontinuous 12% Tricine-polyacrylamide electrophoretic gel (O antigen production was restored in the complemented *wzy*/wzy^+ strain) (15).

The location of the O antigen on the cell surface places it at the interface between the bacterium and its environment (13). Furthermore, the O antigen can extend as far as 30 nm into the surrounding milieu and exhibits some flexibility (12). Because of its prominence and extension into the environment, LPS (more specifically, the O antigen) has been implicated in various stages of microbial pathogenesis in both mammalian and plant systems (11, 14, 15). It can also play a protective role by acting as a barrier against antimicrobial substances and shielding the pathogen from host recognition (16, 17). Furthermore, it acts as a key contributor to bacterial adhesion to host cells (i.e., plant and mammalian cells) or surfaces (10).

In general, bacterial cell surfaces are negatively charged; the magnitude of the charge depends on structures on the cell surface, including LPS (10, 18). In this study, we demonstrate that truncation of the *X. fastidiosa* O antigen causes the cell surface to become significantly more negatively charged than the wild type when cells are grown in defined *X. fastidiosa* medium (XFM) with 0.01% pectin. This change in charge was also observed in a previous study in which the cells were grown in rich PD3 medium (14, 15). In terms of relating O antigen structure and cell surface charge to function, truncation of the O antigen caused by a mutation in *wzy* led to a phenotype of hyperattachment to a glass surface *in vitro*. However, the *wzy* mutant was significantly compromised in the cell-cell aggregation phase of biofilm formation, which resulted in marked changes in the topography and roughness of the mature biofilm *in vitro*. The *wzy* mutant formed a thinner and rougher biofilm than did the wild-type parent, indicating that it could initiate surface attachment but could not build on itself to form a mature biofilm. Consequently, the *wzy* mutant was severely defective in virulence in a susceptible grapevine host (15).

In this study, we demonstrate that the *wzy* mutant is significantly defective in attachment to the insect foregut cuticle, which is essentially the opposite of the hyperattaching phenotype observed *in planta* and *in vitro*. This provides further evidence that the dynamics of biofilm formation are markedly different in the insect environment than in the plant environment, and we establish that the O antigen chain of LPS is a critical modulator of *X. fastidiosa* attachment to the cuticular surface of the BGSS foregut. Furthermore, this defect in attachment halts biofilm formation in the foregut, thus compromising the overall acquisition and retention of *X. fastidiosa* by the BGSS. This highlights LPS as an important mediator of vector acquisition and as a potential target for disruption of *X. fastidiosa* transmission as a means of disease control.

MATERIALS AND METHODS

Bacterial strains and growth conditions. We used wild-type *X. fastidiosa* Temecula1 (19) and a *wzy* mutant strain (15). *X. fastidiosa* Temecula1 wild-type and *wzy* mutant strains were grown for 7 days at 28°C on solid PD3 medium, with or without kanamycin at 5 μg/ml. For acquisition tests, strains were prepared as described previously (20), with slight modifications. In brief, wild-type and *wzy* mutant *X. fastidiosa* cells were harvested from PD3 plates and suspended in liquid XFM. Bacterial cell suspensions were adjusted to an optical density at 600 nm (OD_{600}) of 0.25 (approximately 10^8 cells/ml); 20-μl aliquots of cell suspensions were striped onto XFM with 0.01% pectin. Cells were incubated at 28°C for an additional 7 days and suspended in artificial insect diet solution (containing 0.7 mM L-glutamine, 0.1 mM L-asparagine, and 1 mM sodium citrate [pH 6.4]) (20), and suspensions were adjusted to 10^8 cells/ml (OD_{600} of 0.25).

Insect source and maintenance. Adult blue-green sharpshooters (BGSSs), *Graphocephala atropunctata* (Signoret) (Hemiptera, Cicadellidae), were collected in Laguna Beach, California. Insects were reared on sweet basil (*Ocimum basilicum* L.) under greenhouse conditions (22 ± 5°C). Prior to the assays, subsets of second-generation adults were tested using the quantitative PCR (qPCR) protocol described below, to confirm

that the insects were free of *X. fastidiosa*. Only second-generation adults were used in the acquisition tests.

Insect acquisition experiments. Acquisition experiments using artificial diets were performed as described previously (20), with slight modifications. Insects were caged individually in artificial sachets constructed from the base of a 5-ml pipette tip and sealed with a moist cotton ball. Each replicate consisted of 35 μl of bacterial cell suspension loaded onto a layer of stretched Parafilm, with the drop later being covered with another layer of Parafilm. Insects were given a 6-h acquisition access period (AAP) at 20°C. To remove any unbound cells present in the ingested solutions, insects were transferred to healthy basil plants for a 48-h clearing and multiplication period. Immediately following the 48-h clearing and multiplication period at room temperature, 30 insect heads per treatment were placed in 4% glutaraldehyde fixative for scanning electron microscopy or whole insects were immediately stored at −20°C until DNA extraction and qPCR analysis. For qPCR analysis, 40 insects were exposed to the wild-type bacteria, 36 were exposed to the *wzy* mutant, and 33 were exposed to diet only.

Quantification of *X. fastidiosa*. Following the 48-h clearing and multiplication period, insects were immediately stored at −20°C until further analysis. Genomic DNA extractions were performed with individual BGSS heads by using the Qiagen DNeasy blood and tissue kit (Qiagen, Valencia, CA), with the addition of liquid nitrogen pretreatment. Using a disposable microtube pestle, individual heads were ground to a fine powder with liquid nitrogen. Samples were then processed according to the standard DNeasy protocol, and the resulting DNA was concentrated using a SpeedVac concentrator, prior to use in qPCR. For quantification of *X. fastidiosa* in the insect samples, standard curves were created using a BGSS genomic DNA/*X. fastidiosa* genomic DNA concentration ratio of 2:1 (see Fig. S1 in the supplemental material). To prepare the DNA for determination of the insect sample standard curve, cultured *X. fastidiosa* cells were adjusted to an OD_{600} of 0.25, corresponding to approximately 1×10^8 cells/ml (1×10^5 cells/μl), and genomic DNA was extracted using the Qiagen DNeasy blood and tissue kit (Qiagen, Valencia, CA). The resulting DNA was mixed with insect DNA in a 2:1 concentration ratio. From this mixture, 10-fold serial dilutions were made to create a range of standards from 10,000 to 10 *X. fastidiosa* cells/μl (see Fig. S1 in the supplemental material). Quantitative PCR was performed using a C1000 thermal cycler fitted with a CFX96 real-time PCR detection system (Bio-Rad, Hercules, CA). The TaqMan primers and probe targeting the ITS region of the *X. fastidiosa* Temecula1 genome were as follows: *Xf*ITSF6, 5′-GAGTATGG TGAATATAATTGTC-3′; *Xf*ITSR6, 5′-CAACATAAACCCAAACCTAT-3′; *Xf*ITS6-probe1, 5′-6-FAM-CCAGGCGTCCTCACAAGTTA-black hole quencher 1 (BHQ1)-6-FAM-3′ (BHQ1 was obtained from Eurofins MWG Operon, Huntsville, AL). PCRs were performed in triplicate in a volume of 25 μl and contained 2.5 μl of 10× buffer mix (Qiagen, Valencia, CA), 2.5 μl of $MgCl_2$ buffer (Qiagen, Valencia, CA), 200 μM each deoxynucleoside triphosphate (dNTP) (Qiagen, Valencia, CA), 400 nM each primer, 250 nM probe, 1.25 units of *Taq* DNA polymerase, and 1 μl of sample or standard template. PCRs were performed using an initial denaturation step at 94°C for 5 min followed by 38 cycles of denaturation at 94°C for 20 s, primer annealing at 63°C for 30 s, and primer extension at 72°C for 30 s, with a final extension step at 72°C for 2 min.

Scanning electron microscopy. Using a series of ethanol dilutions, BGSS heads were dehydrated and critical point dried using a Tousimis Autosamdri-815B critical point dryer (Tousimis, Rockville, MD). Foreguts were gently dissected from insect heads and mounted onto copper tape attached to aluminum stubs. Samples were coated in a platinum-palladium mixture using a Cressington 108 auto sputter coater (Cressington Scientific Instruments Ltd., Watford, England) and imaged using a Philips XL30 field emission gun (FEG) scanning electron microscope (FEI, Hillsboro, OR).

Hindwing attachment assay. The attachment assay was conducted according to previously established protocols (21), with slight modifications. Using BGSS adults from the same source colony, hindwings were removed and gently washed in distilled water. Wings were immobilized on water agar plates (1.5%; Becton, Dickinson, and Co., Franklin Lakes, NJ). *X. fastidiosa* wild-type and *wzy* mutant strains were grown as described above. Suspensions were adjusted to an OD_{600} of 0.25, and 2 μl of each suspension was loaded onto individual wings. Hindwings were incubated at 28°C for 6 h, after which suspensions were removed and wings were rinsed gently with distilled water. Each wing was used in a separate DNA extraction, using the Qiagen DNeasy blood and tissue kit (Qiagen, Valencia, CA), and bacterial titers were determined using the qPCR method described above. Experiments consisted of three independent assays with three replicates per strain, totaling nine insects per treatment.

Zeta potential measurements with bacterial cells and sharpshooter hindwings. Zeta potential measurements on *X. fastidiosa* cells were determined using a ZetaPALS analyzer (Brookhaven Instruments Corp., Holtsville, NY). Zeta potential measurements on *X. fastidiosa* cells were performed as described previously (15). All bacterial strains were grown on solid PD3 medium for 7 days, harvested, and suspended in liquid XFM (without filter-sterilized supplement containing L-asparagine, L-cysteine, L-glutamine, and bovine serum albumin). Cell suspensions were adjusted to an OD_{600} of 0.25 (approximately 10^8 cells/ml); 20-μl aliquots of cell suspensions were striped onto XFM with 0.01% pectin. Cells were incubated at 28°C for an additional 7 days, harvested, washed once with 10 mM KCl, and resuspended in 10 mM KCl to a final OD_{600} of 0.2. The electrophoretic mobility of the bacterial cells was determined at 20°C using a ZetaPALS analyzer (Brookhaven Instruments Corp., Holtsville, NY). Experiments consisted of three independent assays with five replicates per strain. Mobility values determined by electrophoresis were converted to zeta potential values (22).

To determine the relative surface charges of BGSS foreguts, streaming potential measurements were conducted on BGSS hindwings. A streaming potential analyzer (SurPASS; Anton Paar, Graz, Austria) with an adjustable gap cell was used to measure the electrokinetic properties of BGSS hindwings (in streaming current mode). Hindwings were immobilized on the sample supports (20 mm by 10 mm) within the cell, and the gap was adjusted to approximately 100 μm. Measurements were made at 25°C using 10 mM KCl (without initial pH adjustment), with a maximal pressure difference of 50 kPa. At each pH increment, measurements were repeated four times. Acid titration (0.05 M HCl) was used to evaluate the surface charge at pH 7.

Hydrophobicity measurements with sharpshooter hindwings. Static contact angle (SCA) measurements of immobilized hindwings were performed using a drop shape analyzer (DSA25; Krüss, Hamburg, Germany). Average contact angles were obtained from measurements at four different points. Using the instrument software, SCA values were calculated using the tangential curve-fitting method, at 10 s after a drop of water (10 μl) had been dropped onto the surface.

DLVO profiles. The Derjaguin-Landau-Verwey-Overbeek (DLVO) theory was applied to further evaluate the relative contributions of electrostatic and van der Waals interactions between the foregut surface and bacteria within the insect (23–25). The van der Waals attraction is governed by a constant, i.e., the Hamaker constant (A), which depends on the material properties. The Hamaker constant used to evaluate the van der Waals interactions between chitin, water, and *X. fastidiosa* was A_{132} of 3×10^{-21} J. This constant (A_{132}) was calculated using the geometric mean (25) of known constants for water (25) and bacteria (26), and the Hamaker constant was determined using the contact angle of the BGSS hindwings (27, 28). Using this information, interaction profiles were developed by assuming sphere-plate geometry (23–25, 29).

Comsol model. Using a commercial finite element package (Comsol Multiphysics v4.3), a computational model was developed to evaluate fluid flow through the sharpshooter foregut. The computational domain used was a two-dimensional longitudinal section through the pharynges. The two-dimensional model provides valuable insights into the dynamic process of sharpshooter feeding and fluid stagnation, which may promote bacterial attachment. However, it is representative of flow conditions only

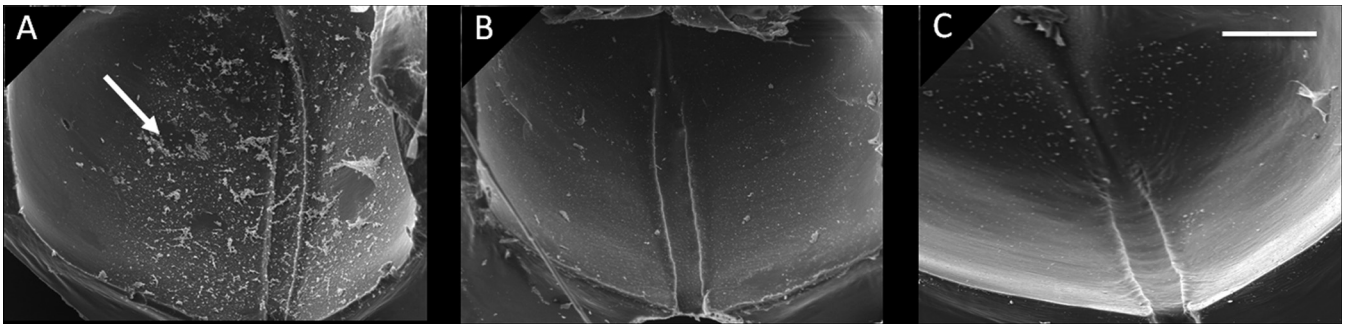

FIG 1 Truncation of the O antigen compromises colonization of the cibarium. The *wzy* mutant had notably reduced ability to attach to the cibarium. Scanning electron micrographs of the hypopharyngeal surface of the cibarium of BGSSs fed on artificial diets containing wild-type *X. fastidiosa* (A), the *wzy* mutant (B), or artificial diet only (C) for 6 h are presented. Images are oriented so that the stylet food canal is at the bottom and the pharynx at the top; thus, ingested fluid would flow inward from bottom to top. Images are representative of 30 total replicates per treatment. Arrow, bacterial aggregates. Diet-fed insects represent negative controls. Bar, 20 μm.

under steady-state laminar flow. The velocity field is described by the equations of motion for an incompressible fluid and the continuity equation. The following boundary conditions were imposed. At the inlet, a fully developed laminar velocity profile was specified, while the outflow boundary was set to constant (atmospheric) pressure. At the foregut surfaces (the upper and lower boundaries), the tangential velocity was set to zero (no-slip conditions). The computational domain was meshed using a structured, boundary-layer-type mesh, with an increasing mesh density near the spacer and membrane surface. This enabled efficient computation while retaining accuracy where the largest concentration variations in the system were expected. Mesh refinement was carried out to ensure the independence of the solution on the mesh. In all simulations, the solution was assumed to be water, with fluid density and dynamic viscosity of 1,000 kg/m^3 and 10^{-3} Pa · s, respectively.

Statistical tests. All experiments were analyzed by one-way analysis of variance (ANOVA), using PROC GLM (SAS Institute) to deal with unequal class sizes. Prior to the ANOVA, data were checked for normality and homogeneity of variance using PROC UNIVARIATE (SAS Institute). All experiments met these criteria. Differences among treatment means were determined by Tukey's honestly significant difference (HSD) test at $P = 0.05$.

RESULTS

O antigen chain length modulates vector acquisition of *X. fastidiosa*. After insects were fed on artificial diet sachets containing wild-type bacteria, BGSS foreguts contained large flocculent microcolonies of bacteria. In *wzy* mutant-fed insects, however, bacterial aggregates were strikingly absent. A few sparse cells were observed throughout the foregut of *wzy* mutant-fed insects, but overall these insects showed almost no visible bacterial colonization in the cibarial and precibarial regions of the foregut and were nearly identical to insects that were exposed to the artificial diet solution control (Fig. 1 and 2).

Quantitatively, sharpshooters that were fed suspensions of the *wzy* mutant harbored significantly fewer cells ($F_{2,39} = 18.29$, $P < 0.01$) than did those that were fed wild-type bacteria (Fig. 3). Numbers of bacterial cells were significantly different between insects fed wild-type *X. fastidiosa* and those exposed to the *wzy* mutant or the artificial diet solution control; the latter two groups were not significantly different. We found that previously designed quantitative PCR (qPCR) primer sets were not able to detect the low *X. fastidiosa* titers within the insects at such an early time point after acquisition. This, in combination with the inhibitory effects of chitin, made initial attempts at *X. fastidiosa* quantification unsuccessful. Therefore, we developed a new TaqMan-

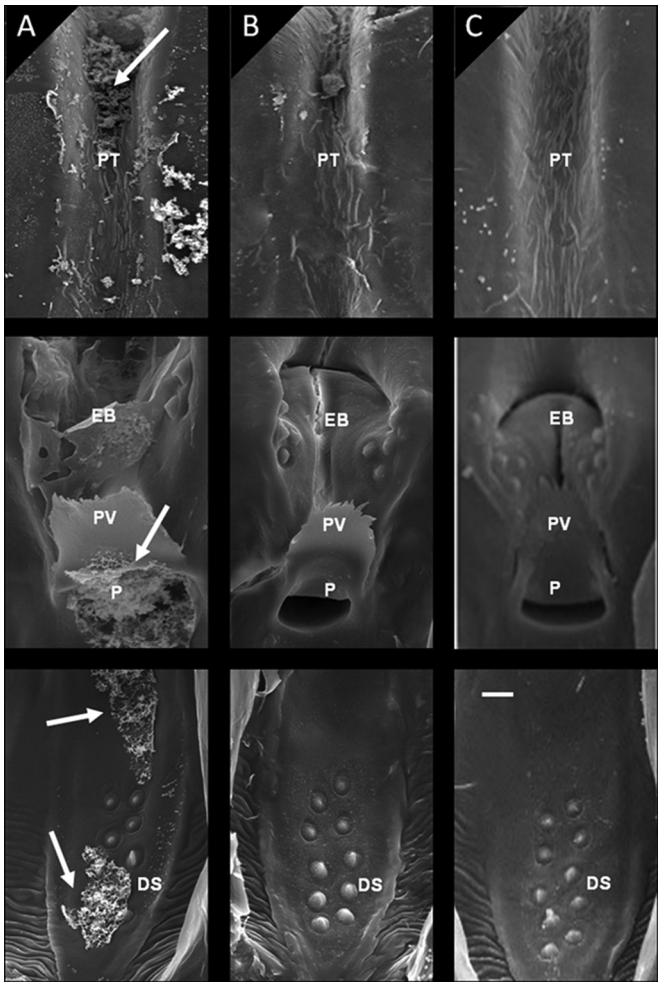

FIG 2 Truncation of the O antigen compromises colonization of the precibarium. The *wzy* mutant had notably reduced ability to attach to all structures within the precibarium, including the distal sensilla, pit, precibarial valve, epipharyngeal basin, and precibarial trough. Scanning electron micrographs of the epipharyngeal surface of the precibarium of BGSSs fed on artificial diets containing wild-type *X. fastidiosa* (A), the *wzy* mutant (B), or artificial diet only (C) for 6 h are presented. The stylet food canal is oriented toward the bottom and the pharynx at the top; thus, ingested fluid would flow inward from bottom to top. Images are representative of 30 total replicates per treatment. Arrows, bacterial aggregates. Diet-fed insects represent negative controls. DS, distal sensilla; P, pit; PV, precibarial valve; EB, epipharyngeal basin; PT, precibarial trough. Bar, 5 μm.

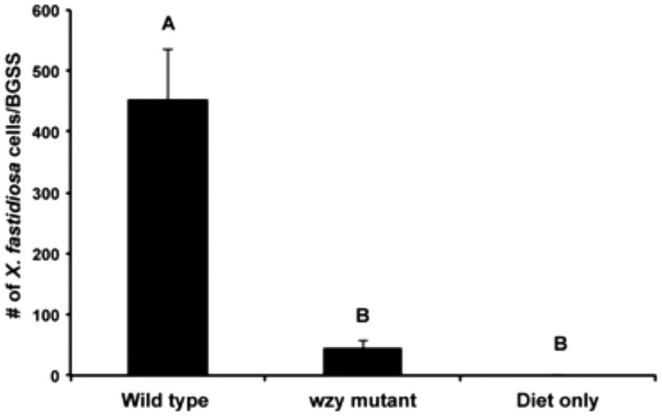

FIG 3 O antigen chain length modulates acquisition by BGSSs. Sharpshooters that were fed on suspensions of the *wzy* mutant had significantly fewer cells adhering to the cuticle than did those that were fed on wild-type bacteria. Inclusion of the BGSS DNA in the standards reduced standard amplification so that the sample amplification curves fell within the range of the standards. No *X. fastidiosa* cells were detected in insects fed solely on diet solution. The graph presents the means of 40, 36, and 33 insects for wild-type, *wzy* mutant, and artificial diet treatments, respectively. Treatments with different letters over the bars were statistically different ($P < 0.01$).

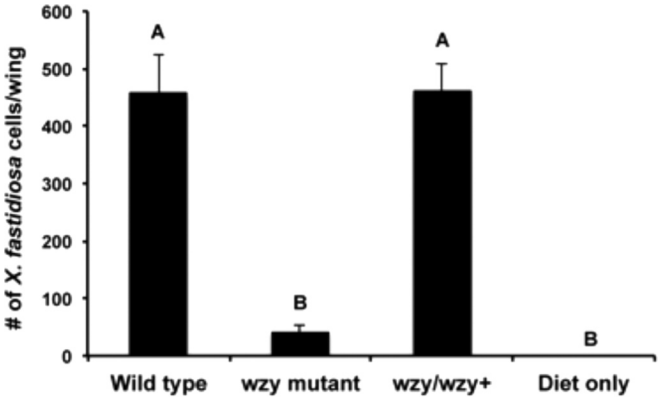

FIG 4 The O antigen mutant is compromised in attachment to BGSS hindwings. The *wzy* mutant cells attached 10-fold less to BGSS hindwings than did wild-type cells. Wild-type cells, *wzy* mutant cells, cells of the *wzy* complemented strain, or a negative control (insect diet solution) were incubated on individual hindwings for 6 h at 28°C. Attached bacterial cells were enumerated using qPCR. The graph presents the mean ± standard error of the mean of nine samples per treatment. Treatments with different letters over the bars were statistically different ($P < 0.0001$).

based protocol for this study that eliminated the laborious removal of inhibitors from insect tissues; instead, we constructed our standard curve using a mixture of BGSS genomic DNA and *X. fastidiosa* genomic DNA to account for inhibitors inherent to the insect samples (see Fig. S1 in the supplemental material).

***In vivo* impaired attachment phenotype is mimicked *ex vivo* on BGSS hindwings.** The sharpshooter foregut is an internal structure, which makes it difficult to perform quantitative measurements of the physiochemical properties of the foregut cuticle. Several studies from other laboratories have deemed sharpshooter hindwings a suitable proxy for both qualitative and quantitative measurements of *X. fastidiosa* interactions with the sharpshooter foregut (6, 21). Using BGSS hindwings, we quantified attachment of *X. fastidiosa* cell suspensions to wings by using qPCR. Both wild-type and *wzy* mutant *X. fastidiosa* cells attached to the hindwings, but the *wzy* mutant was critically impaired in attachment. Significantly fewer (i.e., 10 times fewer) cells of the *wzy* mutant attached, compared with wild-type cells; this phenotype was restored in the complemented *wzy/wzy*$^+$ strain ($F_{11,24} = 13.25$, $P < 0.0001$) (Fig. 4). Thus, the significant impairment that we observed both quantitatively and qualitatively *in vivo* was replicated *ex vivo* with BGSS hindwings, supporting the value of hindwings as a suitable proxy for the foregut cuticular surface (6, 21).

O antigen truncation alters the bacterial cell surface charge. The zeta potential, a measure of cell surface charge, indicated that the *wzy* mutant surface was significantly more negatively charged (−28.6 ± 1.6 mV) than the wild-type surface (−20.6 ± 2.2 mV) ($P < 0.05$) when propagated in XFM with 0.01% pectin (Table 1), which follows the trend observed in other growth media (15). The complemented *wzy/wzy*$^+$ strain had a surface charge (−22.9 ± 1.5 mV) similar to that of wild-type *X. fastidiosa* (statistically insignificant, $P > 0.05$). Using classic Derjaguin-Landau-Verwey-Overbeek (DLVO) theory, which describes the forces between charged surfaces interacting through a liquid medium, we estimated the attractive and repulsive forces between *X. fastidiosa* and the insect cuticular surface. For use in the construction of DLVO profiles, static contact angle (SCA) measurements of immobilized BGSS hindwings were obtained. The SCA of the hindwings was 134 ± 7°. Compared to SCA measurements of other hydrophobic surfaces, such as Teflon (SCA of 110°) (30), this indicated that the hindwing surface is extremely hydrophobic. We made several attempts to calculate the hydrophobicity of the *X. fastidiosa* cells, but their extremely aggregative nature made these experiments difficult to perform. Streaming potential measurements indicated that BGSS hindwings were also negatively charged (−27.4 ± 1.7 mV at pH 7.0) (Table 1). The energy barrier (repulsive force) experienced by *wzy* mutant cells (190.8 kT) was nearly double the barrier experienced by wild-type cells (94.4 kT) (Fig. 5A). Secondary minimum depths (representing a dip in the repulsive force) (Fig. 5B, arrow) and separation distances between BGSS hindwings and the different *X. fastidiosa* strains were calculated (Fig. 5C). The secondary energy minimum for wild-type cells (−5.34 kT) was nearly a full 1 kT deeper than that for *wzy* mutant cells (−4.67 kT) (Fig. 5C), indicating that the wild-type cells have a greater propensity to attach stably to the vector foregut cuticular surface than do *wzy* mutant cells.

Comsol model of velocity magnitude in BGSS foreguts. During ingestion of xylem sap, the cibarial diaphragm (located at the posterior end of the foregut) exhibits a rhythmic motion, powering the piston-like cibarial pump. For convenience, we show the

TABLE 1 Surface charges of *X. fastidiosa* strains and BGSS hindwings, as determined by zeta potential

Sample type	Zeta potential (mV)[a]
Wild-type *X. fastidiosa*	−20.6 ± 2.20 A[b]
wzy mutant *X. fastidiosa*	−28.6 ± 1.64 B
wzy/wzy$^+$ *X. fastidiosa*	−22.9 ± 1.50 A
BGSS hindwings	−27.4 ± 1.67

[a] Mobility values were determined by electrophoresis and converted to zeta potentials. All measurements were taken at pH 7. For bacterial strains, values represent the mean ± standard error of the mean for 15 samples per treatment. For BGSS hindwings, values represent the mean ± standard error of the mean for four biological replicates.
[b] Values followed by different letters are statistically different ($P < 0.01$).

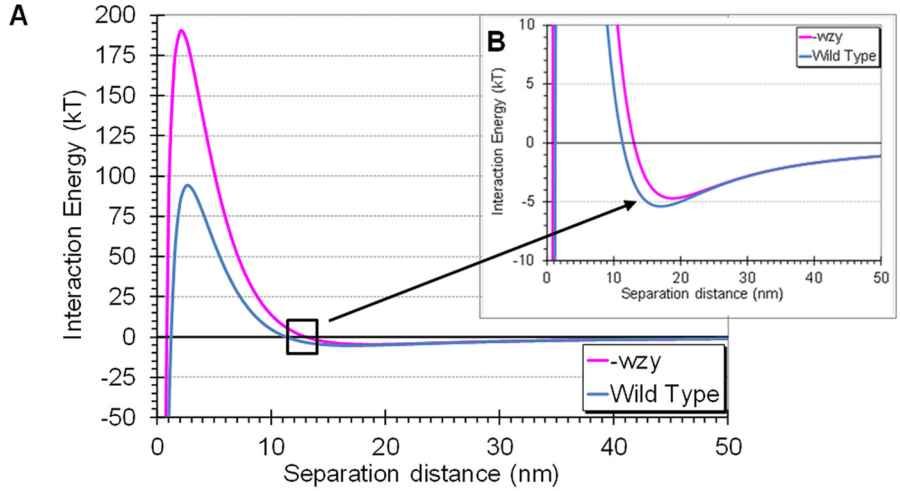

	2nd Energy Min (kT)	Distance (nm)	Energy Barrier (kT)	Distance (nm)
Wild type	-5.34	17	94.4	2.5
wzy mutant	-4.67	19	190.8	2

FIG 5 DLVO profiles of wild-type and *wzy* mutant *X. fastidiosa* strains. (A and B) Profiles displaying primary maximum curves (repulsive force) and secondary minimum curves (dip in the repulsive force) (boxed area in A and enlarged in B, indicated by the arrow) for wild-type and *wzy* mutant cells. The energy barrier experienced by *wzy* mutant cells (190.8 kT) was nearly double the barrier experienced by wild-type cells (94.4 kT). (C) Calculated secondary minimum depths and separation distances between BGSS hindwings and the different *X. fastidiosa* strains. The secondary energy minimum for wild-type cells (−5.34 kT) was nearly a full 1 kT deeper than that for *wzy* mutant cells (−4.67 kT), indicating a stronger dip in the repulsive force.

diaphragm in a semicontracted position within the cibarium (Fig. 6). Figure 6 presents a two-dimensional simulation of the fluid flow within the foregut. The bulk fluid flow of xylem sap through the precibarium is reported to exceed 100 to 500 mm/s during active ingestion, depending on the sharpshooter species (31–33). Here we show that the maximal velocity (V_{max}) within the precibarium of BGSSs exceeds 70 mm/s, exhibiting significant shear force that reduces the probability of bacterial attachment. Due to the significant expansion within the cibarium, the V_{max} rapidly drops to nearly 5 mm/s. At 15 μm proximal to the opening of the cibarium, the shear rate decreases approximately 1,000-fold from that within the precibarium, indicating that the cibarium has areas of stagnation (Fig. 6, blue areas) that would favor initial bacterial attachment.

Areas of *X. fastidiosa* localization within the cibarium support predicted colonization sites determined by the Comsol model. Scanning electron micrographs of BGSS foreguts following artificial feeding of wild-type *X. fastidiosa* and a 6-day clearing and multiplication period revealed the presence of robust *X. fastidiosa* biofilms localized along the outer regions of the cibarium, which supports our Comsol model indicating that bacterial cells could more easily attach to the outer areas of the cibarium, compared to other regions of the foregut (Fig. 7).

DISCUSSION

Acquisition of bacteria by insect vectors depends heavily on the properties of the bacterial cell surface, because it is the first surface to interact with the surrounding environment and thus plays an important role in cell-cell and host-microbe interactions (10, 12). Bacteria have evolved surface-associated polysaccharides, namely, LPS and EPS, that aid in attachment, protection, and survival under pressures exerted by the specific host environments. In insect and plant hosts, *X. fastidiosa* seemingly follows the canonical steps involved in biofilm formation, i.e., initial attachment to the surface followed by aggregation/microcolony formation, macrocolony formation, and biofilm maturation. For *X. fastidiosa*, immunologically based microscopy studies indicated that very sparse amounts of EPS are associated with the cells during the initial attachment phase, with the bulk of the EPS being produced during the late phase of biofilm maturation; substantial amounts can be seen intercalating the biofilm matrix of a mature biofilm (34). This effectively places LPS as the most prominently exposed polysaccharide during the early phases of biofilm formation (15). Therefore, LPS (more specifically, O antigen) likely functions as the first point of contact in attachment to a surface, effectively acting as a primary liaison between *X. fastidiosa* and its hosts. Thus, the structure of O antigen can exert a powerful influence on the critical early stages of attachment. It is known that O antigen plays a role in plant and animal host colonization in bacterial pathosystems (15, 35–38). However, the role of O antigen in insect vector-pathogen interactions has been largely unexplored. In this study, we link O antigen structure to function in the context of attachment to the foregut cuticle and insect acquisition in the *X. fastidiosa* pathosystem.

Our study focused on the role of O antigen in the initial attachment steps of biofilm formation, which is crucial to the acquisition of *X. fastidiosa* by BGSSs. *In vivo*, wild-type *X. fastidiosa* adhered to the foregut with titers of approximately 450 cells/BGSS, following a 6-h AAP on an artificial diet sachet and a 48-h multiplication and clearing period on basil plants (a non-*X. fastidiosa* host). In con-

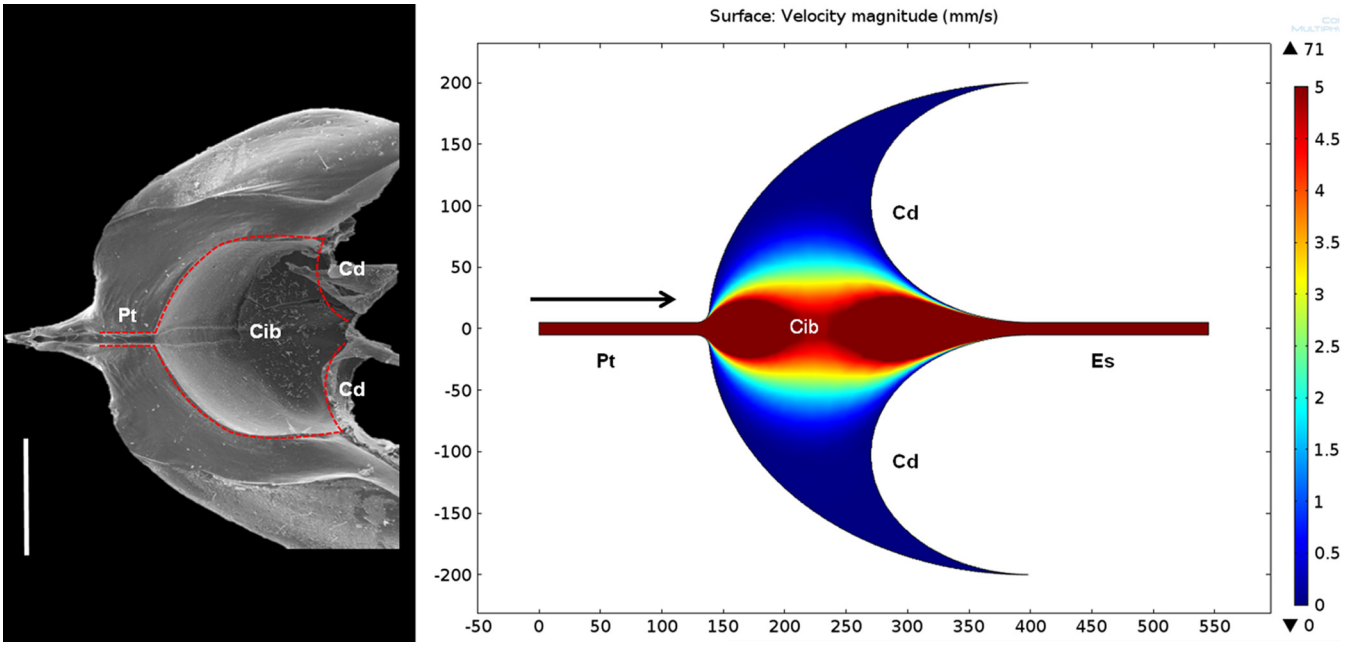

FIG 6 Comsol model representing the hydrodynamics of xylem sap flow during ingestion. The precibarial trough and the central regions of the cibarium experience the greatest sheer hydrodynamic forces, as indicated by the gradient. Dark red areas, flow rates greater than 50 mm/s. Blue areas, areas of stagnation, occurring primarily in the outer regions of the cibarium. Arrow, direction of fluid flow. The figure represents a longitudinal section of the pharynges and is oriented so that the stylet food canal would be to the left and the esophagus to the right. The cibarial diaphragm is shown in a semicontracted position. The model focused specifically on the areas proximal to the epipharyngeal basin, as indicated by the dotted red outline in the left panel. Pt, precibarial trough; Cib, cibarium; Cd, cibarial diaphragm; Es, esophagus. Bar, 200 μm. The *x* and *y* axes are in micrometers.

trast, the *wzy* mutant was compromised in initial adherence to the insect foregut and was present with titers of approximately 45 cells/BGSS. Electron micrographs of the foreguts of BGSSs fed on the artificial diet sachets indicated that the *wzy* mutant sparsely colonized both the cibarial and precibarial areas of the foregut, whereas the wild type thoroughly colonized both of these areas. Thus, based on both quantitative and qualitative data, we demonstrated that truncation of the O antigen resulted in poor adherence of the bacterium to insect foreguts during the early stages of the acquisition process. This defective attachment phenotype was replicated on BGSS hindwings, which is an established tool used to mimic the *X. fastidiosa* binding sites within the insect foregut. Our findings corroborate data from other laboratories that have deemed sharpshooter hindwings a suitable proxy for both qualitative and quantitative measurements of *X. fastidiosa* interactions with the sharpshooter foregut (6, 21, 39). In addition, Killiny and Almeida confirmed the specificity of the *X. fastidiosa*-sharpshooter hindwing interaction, because only *X. fastidiosa* was capable of binding to the hindwings and other Gram-negative bacterial plant pathogens, such as *Pseudomonas syringae* pv. syringae, *Erwinia herbicola*, and *Xanthomonas campestris* pv. campestris, did not attach to the hindwings (6).

Little is known about the influence of electrostatic interactions on bacterial attachment to vector surfaces. This prompted us to characterize both the *X. fastidiosa* cell surface and the insect cuticular surface. For *in vitro* attachment and electrokinetic studies, we used BGSS hindwings as a proxy system to determine how the wild type and the *wzy* mutant interact with the foregut cuticle. From those measurements, we extrapolated the electrostatic repulsive and attractive forces between those two entities using DLVO theory. By performing zeta potential and static contact angle measurements, we found that BGSS hindwings have an overall negative charge and are extremely hydrophobic (even more hydrophobic than Teflon). *X. fastidiosa* is negatively charged, as are most pathogenic bacteria (15). Interestingly, truncation of the *X. fastidiosa* O antigen significantly affected the zeta potential of the bacterial cell surface in the XFM-pectin growth medium and caused the *wzy* mutant to become significantly more negatively charged than the wild-type parent. In relation to the zeta potential of the hindwings (−27.4 mV), there is stronger electrostatic repulsion between the *wzy* mutant (−28.6 mV) and the insect cuticular surface (due to the similarity in charge) than between wild-type *X. fastidiosa* (−20.6 mV) and the insect cuticle. Therefore, on the basis of attractive electrostatic interactions, the wild-type cells (containing fully polymerized O antigen) have a greater propensity to attach to the cuticle.

Bacterial attachment to surfaces can be further modeled using classic DLVO theory, which serves to model particle (bacterial cell) stability (40). It describes the forces between charged surfaces as they interact in a liquid environment (41). Specifically, the overall long-range interaction between two surfaces is composed of two additive forces, namely, electrostatic interactions and van der Waals attraction (41). The Hamaker constant was developed, as discussed previously, to account for the specific bacterium-water-insect cuticle interactions for our environmental conditions and interacting constituents. Hamaker constant calculations define the strength of the attractive van der Waals forces between a particle and a specific surface, and specific constants can be calculated based on the individual constituents of an interaction (42). Using these variables, the resulting DLVO profiles (present-

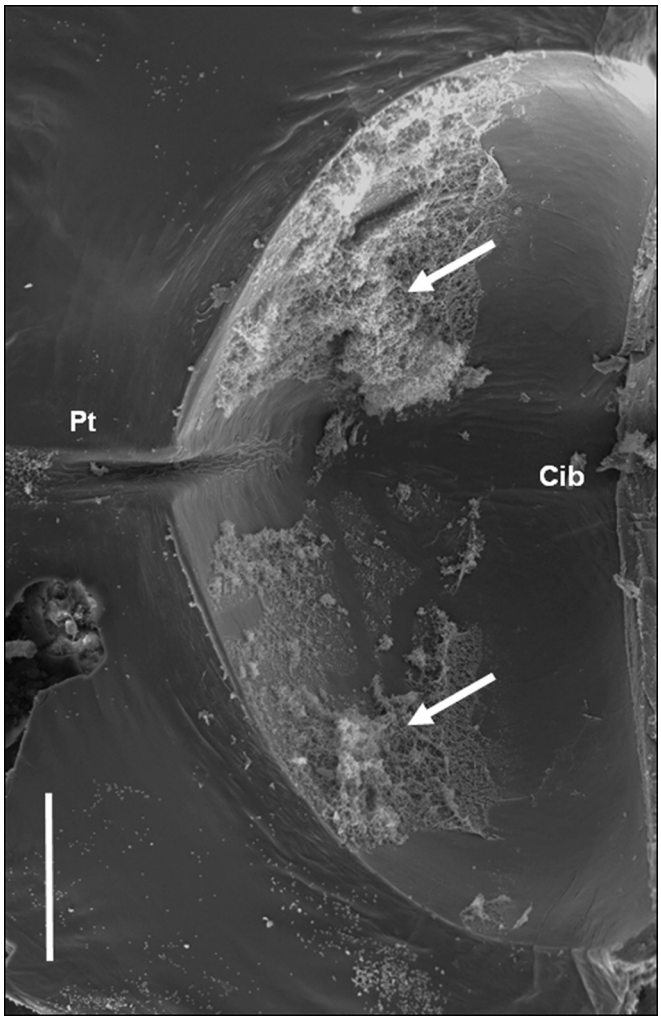

FIG 7 Localization of *X. fastidiosa* in the cibarium supports the Comsol model of predicted areas of colonization. As indicated in the Comsol model, scanning electron micrographs confirm that the ultimate site of *X. fastidiosa* retention is in the cibarium, specifically in the outer regions where stagnation occurs. The figure represents a longitudinal section of the pharynges and is oriented so that the stylet food canal would be to the left and the esophagus to the right. The image is representative of 15 total replicates. Arrows, wild-type *X. fastidiosa* biofilm. Pt, precibarial trough; Cib, cibarium. Bar, 200 μm.

ing the magnitude of interaction energy [kT] between the surfaces versus the separation distance [in nanometers]) for wild-type and *wzy* mutant *X. fastidiosa* strains revealed the existence of a substantial energy barrier between the *wzy* mutant and the insect cuticle (190.8 *kT*), which was approximately double the energy barrier between wild-type *X. fastidiosa* and the insect cuticle (94.4 kT) (as indicated by the primary maximum curves in Fig. 5A). This demonstrates that truncation of the O antigen notably increases the repulsion between the cell and the insect cuticular surface, indicating that *wzy* mutant cells would have a greater challenge in overcoming this energy barrier to allow the attractive van der Waals forces to dominate for attachment to the foregut cuticle. Consequently, less force is required to remove or to dislodge these cells, compared with wild-type cells, which supports our findings that *wzy* mutant cells have difficulty binding to the insect cuticle, both quantitatively and qualitatively.

Overall, the large energy barriers for both the wild-type and *wzy* mutant strains suggest that bacterial attachment is unlikely in the primary maxima. Specifically, the maximal height of the primary maximum curves indicates that *X. fastidiosa* cells, in general, have a considerable energy barrier to overcome to connect to and to attach to the insect cuticular surface but they can still do this effectively. A closer inspection of the DLVO profiles indicated the presence of a substantial secondary energy minimum curve (Fig. 5B), representing a reversible dip in the repulsive force, for the wild-type cells that was nearly a full 1 kT deeper than that for the *wzy* mutant cells (Fig. 5C). Bacterial cells can associate with and adhere to a surface while experiencing the relatively low-level interaction force within the secondary energy minimum (10). This dip in the overall repulsive force, although representing a weak interaction, likely allows the long-chain O antigen of wild-type cells to approach and to interact with the insect surface and act as a tether, thereby facilitating stable deposition of the *X. fastidiosa* cell onto the cuticle. The strength of the interaction in this secondary energy minimum may be weak, but it is sufficiently stable to allow for initial attachment via the O antigen and subsequently for other proteinaceous bacterial adhesins and EPS to reinforce attachment to the foregut surface as the biofilm develops (10).

In order to understand more comprehensively the O antigen-modulated process of vector acquisition of *X. fastidiosa*, we combined information gleaned from the quantification of electrostatic interactions (and particle stability) with fluid flow throughout the BGSS foregut, using a Comsol model. Using this model, we estimated that the wall shear rate within the precibarium, or the rate at which progressive shearing deformation is applied to the fluid (measured in reciprocal seconds), can exceed 25,000 s^{-1} during active ingestion, with the maximum velocity exceeding 70 mm/s at a cross-flow velocity of 5 mm/s. Because the velocity increases rapidly, the shear rate is high. Interestingly, the model predicted prominent areas of stagnation within the outer regions of the cibarium (Fig. 6, blue areas). During ingestion, the strong shear hydrodynamic forces occurring in the precibarium significantly reduce the initial probability that the cells will attach to the precibarium before they are washed away, during either swallowing (fluid flow through the precibarium and past the cibarium into the pharynx) or egestion (expulsion of fluid back out the stylets). Thus, in accordance with our model, the cibarium would be an easier site in which to attach initially (via the O antigen tether) and to remain attached within the foregut, in contrast to the precibarium, which is extremely turbulent.

We speculate that *X. fastidiosa* initially attaches to the cibarium and, as the bacteria multiply and migrate across the cibarial surface to form microcolonies and mature biofilms, the bacteria push into the precibarium, from which they can then become dislodged and inoculated into plants. The mechanism of migration from the cibarium to the precibarium is unknown but could be partially attributed to type IV pilus-driven twitching motility, which facilitates the migration of *X. fastidiosa* against the fluid flow *in planta* (43). In research investigating spatial colonization patterns of *X. fastidiosa* over typical acquisition access periods, Backus and Morgan demonstrated that the initial site of colonization likely occurs in the cibarium, which then acts as a stable reservoir from which *X. fastidiosa* can load progressively into the distal portions of the precibarium (4). Indeed, the presence of *X. fastidiosa* in the precibarium is highly correlated with inoculation of grapevines (44). Our scanning electron micrographs (of BGSS foreguts fed

solely on wild-type *X. fastidiosa*) further substantiated our model, because robust biofilms were more often associated with the outer regions of the cibarium, where less shear force is predicted to occur (Fig. 7). We acknowledge that this initial model is a simplified anatomical representation of the BGSS foregut and the results presented here are representative of insects that have fed on artificial diets. In future studies, we will focus on fine-tuning the model to further our understanding of the fluid dynamics in the foregut. Expanding the studies to other sharpshooter species that serve as vectors for *X. fastidiosa*, as well as allowing insects to acquire the bacteria directly from infected plants, is also warranted.

ACKNOWLEDGMENTS

Funding for this project was provided by the California Department of Food and Agriculture Pierce's Disease and Glassy-Winged Sharpshooter Program. This material is based on work supported by the National Institute of Food and Agriculture, U.S. Department of Agriculture, under award 2013-67012-21277 (awarded to Nichola Kinsinger).

We thank Matt Daugherty for helpful discussions and Crystal M. Johnston (University of California, Riverside) for providing the sharpshooters used in this study. We thank the Central Facility for Microscopy and Microanalysis at the University of California, Riverside, where scanning electron microscopy was performed. We thank Jiue-In Yang (National Taiwan University) for qPCR primers and probe design.

Mention of trade names or commercial products in this publication is solely for the purpose of providing specific information and does not imply recommendation or endorsement by the U.S. Department of Agriculture.

REFERENCES

1. **Lemon SM, Sparling PF, Hamburg MA, Relman DA, Choffnes ER, Mack A, Sparling F.** 2008. Vector-borne diseases: understanding the environmental, human health, and ecological connections: workshop summary. National Academies Press, Washington, DC.
2. **Chen AYS, Walker GP, Carter D, Ng JCK.** 2011. A virus capsid component mediates virion retention and transmission by its insect vector. Proc Natl Acad Sci U S A **108:**16777–16782. http://dx.doi.org/10.1073/pnas.1109384108.
3. **Chatterjee S, Almeida RPP, Lindow S.** 2008. Living in two worlds: the plant and insect lifestyles of *Xylella fastidiosa*. Annu Rev Phytopathol **46:**243–271. http://dx.doi.org/10.1146/annurev.phyto.45.062806.094342.
4. **Backus EA, Morgan DJW.** 2011. Spatiotemporal colonization of *Xylella fastidiosa* in its vector supports the role of egestion in the inoculation mechanism of foregut-borne plant pathogens. Phytopathology **101:**912–922. http://dx.doi.org/10.1094/PHYTO-09-10-0231.
5. **Killiny N, Almeida RPP.** 2014. Factors affecting the initial adhesion and retention of the plant pathogen *Xylella fastidiosa* in the foregut of an insect vector. Appl Environ Microbiol **80:**420–426. http://dx.doi.org/10.1128/AEM.03156-13.
6. **Killiny N, Almeida RPP.** 2009. *Xylella fastidiosa* afimbrial adhesins mediate cell transmission to plants by leafhopper vectors. Appl Environ Microbiol **75:**521–528. http://dx.doi.org/10.1128/AEM.01921-08.
7. **Killiny N, Martinez RH, Dumenyo CK, Cooksey DA, Almeida RPP.** 2013. The exopolysaccharide of *Xylella fastidiosa* is essential for biofilm formation, plant virulence, and vector transmission. Mol Plant Microbe Interact **26:**1044–1053. http://dx.doi.org/10.1094/MPMI-09-12-0211-R.
8. **Dinglasan RR, Jacobs-Lorena M.** 2005. Insight into a conserved lifestyle: protein-carbohydrate adhesion strategies of vector-borne pathogens. Infect Immun **73:**7797–7807. http://dx.doi.org/10.1128/IAI.73.12.7797-7807.2005.
9. **Caroff M, Karibian D.** 2003. Structure of bacterial lipopolysaccharides. Carbohydr Res **338:**2431–2447. http://dx.doi.org/10.1016/j.carres.2003.07.010.
10. **Walker SL, Redman JA, Elimelech M.** 2004. Role of cell surface lipopolysaccharides in *Escherichia coli* K12 adhesion and transport. Langmuir **20:**7736–7746. http://dx.doi.org/10.1021/la049511f.
11. **Lerouge I, Vanderleyden J.** 2002. O-antigen structural variation: mechanisms and possible roles in animal/plant-microbe interactions. FEMS Microbiol Rev **26:**17–47. http://dx.doi.org/10.1111/j.1574-6976.2002.tb00597.x.
12. **Clements A, Gaboriaud F, Duval JFL, Farn JL, Jenney AW, Lithgow T, Wijburg OLC, Hartland EL, Strugnell RA.** 2008. The major surface-associated saccharides of *Klebsiella pneumoniae* contribute to host cell association. PLoS One **3:**e3817. http://dx.doi.org/10.1371/journal.pone.0003817.
13. **Raetz CRH, Whitfield C.** 2002. Lipopolysaccharide endotoxins. Annu Rev Biochem **71:**635. http://dx.doi.org/10.1146/annurev.biochem.71.110601.135414.
14. **Zhang L, Radziejewska-Lebrecht J, Krajewska-Pietrasik D, Toivanen P, Skurnik M.** 1997. Molecular and chemical characterization of the lipopolysaccharide O-antigen and its role in the virulence of *Yersinia enterocolitica* serotype O:8. Mol Microbiol **23:**63–76. http://dx.doi.org/10.1046/j.1365-2958.1997.1871558.x.
15. **Clifford JC, Rapicavoli JN, Roper MC.** 2013. A rhamnose-rich O-antigen mediates adhesion, virulence, and host colonization for the xylem-limited phytopathogen *Xylella fastidiosa*. Mol Plant Microbe Interact **26:**676–685. http://dx.doi.org/10.1094/MPMI-12-12-0283-R.
16. **Pel MJC, Pieterse CMJ.** 2013. Microbial recognition and evasion of host immunity. J Exp Bot **64:**1237–1248. http://dx.doi.org/10.1093/jxb/ers262.
17. **Silipo A, Molinaro A, Sturiale L, Dow JM, Erbs G, Lanzetta R, Newman M-A, Parrilli M.** 2005. The elicitation of plant innate immunity by lipo-oligosaccharide of *Xanthomonas campestris*. J Biol Chem **280:**33660–33668. http://dx.doi.org/10.1074/jbc.M506254200.
18. **Wilson WW, Wade MM, Holman SC, Champlin FR.** 2001. Status of methods for assessing bacterial cell surface charge properties based on zeta potential measurements. J Microbiol Methods **43:**153–164. http://dx.doi.org/10.1016/S0167-7012(00)00224-4.
19. **Guilhabert MR, Hoffman LM, Mills DA, Kirkpatrick BC.** 2001. Transposon mutagenesis of *Xylella fastidiosa* by electroporation of Tn5 synaptic complexes. Mol Plant Microbe Interact **14:**701–706. http://dx.doi.org/10.1094/MPMI.2001.14.6.701.
20. **Killiny N, Almeida RPP.** 2009. Host structural carbohydrate induces vector transmission of a bacterial plant pathogen. Proc Natl Acad Sci U S A **106:**22416–22420. http://dx.doi.org/10.1073/pnas.0908562106.
21. **Killiny N, Prado SS, Almeida RPP.** 2010. Chitin utilization by the insect-transmitted bacterium *Xylella fastidiosa*. Appl Environ Microbiol **76:**6134–6140. http://dx.doi.org/10.1128/AEM.01036-10.
22. **O'Brien RW, White LR.** 1978. Electrophoretic mobility of a spherical colloidal particle. J Chem Soc Faraday Trans 2 **74:**1607–1626.
23. **Chowdhury I, Hong Y, Honda RJ, Walker SL.** 2011. Mechanisms of TiO_2 nanoparticle transport in porous media: role of solution chemistry, nanoparticle concentration, and flowrate. J Colloid Interface Sci **360:**548–555. http://dx.doi.org/10.1016/j.jcis.2011.04.111.
24. **Hong Y, Honda RJ, Myung NV, Walker SL.** 2009. Transport of iron-based nanoparticles: role of magnetic properties. Environ Sci Technol **43:**8834–8839. http://dx.doi.org/10.1021/es9015525.
25. **Gregory J.** 2005. Particles in water: properties and processes. CRC Press, Boca Raton, FL.
26. **Redman JA, Walker SL, Elimelech M.** 2004. Bacterial adhesion and transport in porous media: role of the secondary energy minimum. Environ Sci Technol **38:**1777–1785. http://dx.doi.org/10.1021/es034887l.
27. **Janjaroen D, Ling F, Monroy G, Derlon N, Mogenroth E, Boppart SA, Liu W-T, Nguyen TH.** 2013. Roles of ionic strength and biofilm roughness on adhesion kinetics of *Escherichia coli* onto groundwater biofilm grown on PVC surfaces. Water Res **47:**2531–2542. http://dx.doi.org/10.1016/j.watres.2013.02.032.
28. **Van Oss CJ.** 1993. Acid-base interfacial interactions in aqueous media. Colloids Surf A Physicochem Eng Asp **78:**1–49. http://dx.doi.org/10.1016/0927-7757(93)80308-2.
29. **Hogg R, Healy TW, Fuerstenau DW.** 1966. Mutual coagulation of colloidal dispersions. Trans Faraday Soc **62:**1638–1651. http://dx.doi.org/10.1039/tf9666201638.
30. **Goswami S, Klaus S, Benziger J.** 2008. Wetting and absorption of water drops on Nafion films. Langmuir **24:**8627–8633. http://dx.doi.org/10.1021/la800799a.
31. **Purcell AH, Hopkins DL.** 1996. Fastidious xylem-limited bacterial plant pathogens. Annu Rev Phytopathol **34:**131–151. http://dx.doi.org/10.1146/annurev.phyto.34.1.131.
32. **Purcell AH, Finlay AH, McLean DL.** 1979. Pierce's disease bacterium:

mechanism of transmission by leafhopper vectors. Science **206:**839–841. http://dx.doi.org/10.1126/science.206.4420.839.
33. **Andersen PC, Brodbeck BV, Mizell RF.** 1992. Feeding by the leafhopper, *Homalodisca coagulata*, in relation to xylem fluid chemistry and tension. J Insect Physiol **38:**611–622. http://dx.doi.org/10.1016/0022-1910(92)90113-R.
34. **Roper MC, Greve LC, Labavitch JM, Kirkpatrick BC.** 2007. Detection and visualization of an exopolysaccharide produced by *Xylella fastidiosa* in vitro and in planta. Appl Environ Microbiol **73:**7252–7258. http://dx.doi.org/10.1128/AEM.00895-07.
35. **Petrocelli S, Tondo ML, Daurelio LD, Orellano EG.** 2012. Modifications of *Xanthomonas axonopodis* pv. citri lipopolysaccharide affect the basal response and the virulence process during citrus canker. PLoS One **7:**e40051. http://dx.doi.org/10.1371/journal.pone.0040051.
36. **Barak JD, Jahn CE, Gibson DL, Charkowski AO.** 2007. The role of cellulose and O-antigen capsule in the colonization of plants by *Salmonella enterica*. Mol Plant Microbe Interact **20:**1083–1091. http://dx.doi.org/10.1094/MPMI-20-9-1083.
37. **Boyer RR, Sumner SS, Williams RC, Kniel KE, McKinney JM.** 2011. Role of O-antigen on the *Escherichia coli* O157:H7 cells hydrophobicity, charge and ability to attach to lettuce. Int J Food Microbiol **147:**228–232. http://dx.doi.org/10.1016/j.ijfoodmicro.2011.04.016.
38. **Bengoechea JA, Najdenski H, Skurnik M.** 2004. Lipopolysaccharide O-antigen status of *Yersinia enterocolitica* O:8 is essential for virulence and absence of O-antigen affects the expression of other *Yersinia* virulence factors. Mol Microbiol **52:**451–469. http://dx.doi.org/10.1111/j.1365-2958.2004.03987.x.
39. **Baccari C, Killiny N, Ionescu M, Almeida RPP, Lindow SE.** 2014. Diffusible signal factor-repressed extracellular traits enable attachment of *Xylella fastidiosa* to insect vectors and transmission. Phytopathology **104:**27–33. http://dx.doi.org/10.1094/PHYTO-06-13-0151-R.
40. **Fennema OR.** 1996. Food chemistry, 3rd ed, p 115–116. Marcel-Dekker, Inc., New York, NY.
41. **Ravina L, Moramarco N.** 1993. Everything you want to know about coagulation & flocculation. Zeta-Meter, Inc., Staunton, VA.
42. **Hermansson M.** 1999. The DLVO theory in microbial adhesion. Colloids Surf B Biointerfaces **14:**105–119. http://dx.doi.org/10.1016/S0927-7765(99)00029-6.
43. **Meng Y, Li Y, Galvani CD, Hao G, Turner JN, Burr TJ, Hoch H.** 2005. Upstream migration of *Xylella fastidiosa* via pilus-driven twitching motility. J Bacteriol **187:**5560–5567. http://dx.doi.org/10.1128/JB.187.16.5560-5567.2005.
44. **Almeida RPP, Purcell AH.** 2006. Patterns of *Xylella fastidiosa* colonization on the precibarium of sharpshooter vectors relative to transmission to plants. Ann Entomol Soc Am **99:**884–890. http://dx.doi.org/10.1603/0013-8746(2006)99[884:POXFCO]2.0.CO;2.